Available online at www.sciencedirect.com

ScienceDirect

Neuromuscular Disorders 31 (2021) 348–358

www.elsevier.com/locate/nmd

Functional analysis of a novel POLγA mutation associated with a severe perinatal mitochondrial encephalomyopathy

Niklas Darin[a,1,*], Triinu Siibak[b,1], Bradley Peter[b], Carola Hedberg-Oldfors[c], Gittan Kollberg[c], Vassili Kalbin[b], Ali-Reza Moslemi[c], Bertil Macao[b], Anders Oldfors[c], Maria Falkenberg[b,*]

[a] Department of Pediatrics, Institute of Clinical Sciences, University of Gothenburg, Gothenburg, Sweden
[b] Department of Medical Biochemistry and Cell Biology, Institute of Biomedicine, University of Gothenburg, Box 440, 40530 Gothenburg, Sweden
[c] Department of Laboratory Medicine, Institute of Biomedicine, University of Gothenburg, Gothenburg, Sweden

Received 12 October 2020; received in revised form 5 January 2021; accepted 6 January 2021

Abstract

Mutations in the mitochondrial DNA polymerase gamma catalytic subunit (POLγA) compromise the stability of mitochondrial DNA (mtDNA) by leading to mutations, deletions and depletions in mtDNA. Patients with mutations in POLγA often differ remarkably in disease severity and age of onset. In this work we have studied the functional consequence of POLγA mutations in a patient with an uncommon and a very severe disease phenotype characterized by prenatal onset with intrauterine growth restriction, lactic acidosis from birth, encephalopathy, hepatopathy, myopathy, and early death. Muscle biopsy identified scattered COX-deficient muscle fibers, respiratory chain dysfunction and mtDNA depletion. We identified a novel POLγA mutation (p.His1134Tyr) in *trans* with the previously identified p.Thr251Ile/Pro587Leu double mutant. Biochemical characterization of the purified recombinant POLγA variants showed that the p.His1134Tyr mutation caused severe polymerase dysfunction. The p.Thr251Ile/Pro587Leu mutation caused reduced polymerase function in conditions of low dNTP concentration that mimic postmitotic tissues. Critically, when p.His1134Tyr and p.Thr251Ile/Pro587Leu were combined under these conditions, mtDNA replication was severely diminished and featured prominent stalling. Our data provide a molecular explanation for the patients mtDNA depletion and clinical features, particularly in tissues such as brain and muscle that have low dNTP concentration.

Keywords: DNA polymerase γ; Mutation; Mitochondrial replication; Disease; Perinatal phenotype.

1. Introduction

DNA polymerase gamma (POLγ) is a nuclear-encoded protein that replicates mitochondrial DNA (mtDNA). Human POLγ is a heterotrimer comprising the catalytic POLγA subunit and a dimeric POLγB processivity factor [1]. POLγA has 5′−3′ DNA polymerase and 3′−5′ exonuclease activities, maintaining a relatively constant mtDNA copy number [1,2]. Mutations in the gene encoding POLγA (*POLG*) are a common cause of mitochondrial disease, with over 300 causative mutations reported [3] (https://tools.niehs.nih.gov/polg/). Defects in replication can cause mtDNA depletion, deletions and point mutations, leading to oxidative phosphorylation impairment, mitochondrial dysfunction and disease [3-5].

The clinical spectrum of POLγ-related disorders is broadly subdivided into three age-dependent phenotypes: (1) adulthood-onset autosomal dominant or recessive chronic progressive external ophthalmoplegia (CPEO: MIM 157,640 and 258,450); (2) adolescence-onset sensory ataxic neuropathy, dysarthria and ophthalmoparesis (SANDO: MIM 607,459) or spinocerebellar ataxia-epilepsy (SCAE: MIM 607,459); and (3) infancy/early childhood-onset Alpers

* Corresponding authors.
E-mail addresses: niklas.darin@vgregion.se (N. Darin), maria.falkenberg@medkem.gu.se (M. Falkenberg).
[1] These authors contributed equally to this work.

https://doi.org/10.1016/j.nmd.2021.01.004

syndrome (MIM 203,700), characterized by a severe hepatocerebral syndrome [6-9]. In this study we identified a patient with a unique and severe perinatal phenotype due to a novel p.His1134Tyr mutation in the *POLG* gene in *trans* with the common p.Thr251Ile/Pro587Leu double mutant. Intrauterine onset with early fatal phenotype has, to our knowledge, only been described in one previous individual with POLγ-related disease characterized by myopathy and gastrointestinal pseudo obstruction [10].

The aim of this study was to ascribe a molecular role for the novel POLγA p.His1134Tyr mutation in combination with the common p.Thr251Ile/Pro587Leu double mutant using clinical and laboratory investigations, and *in vitro* biochemical characterization of the mutant proteins.

2. Material and methods

2.1. Patient description

The boy was the first child of healthy unrelated parents with no family history of neurological disease. The mother was healthy during pregnancy, which was complicated by intrauterine growth restriction of 35%, and birth was by cesarian section after 38+2 weeks of gestation (normal ~ 40 weeks). Birth weight was 2380 g (- 2.5 SD), length was 47 cm (- 1.5 SD) and head circumference was 33 cm (- 1 SD). The APGAR score was normal (9–10–10). From the first day of life the boy was severely floppy with sucking difficulties requiring tube feeding. During the first week of age, blood lactate levels were increased up to 7–8 mmol/L (ref. v. <1.8) with pH 7.32 (ref. v. 7.35–7.45) and Base excess at −5 (ref. v. −3 – 3). The serum creatine kinase level (S-CK) was elevated at 1616 IU/L (ref.v. <170). The results from the polarography and spectrophotometry in isolated mitochondria were in the lower range of the controls but considered normal for a child as young as two weeks of age. A TORCH-screen showed IgG-antibodies against Toxoplasma Gondii, CMV and Parvovirus that were considered to have maternal origin. Mild anemia due to AO-immunization required blood transfusion, and a mild hypocalcemia was normalized upon calcium supplementation. Clinical examination revealed the absence of eye contact, infolded thumbs, backward bending of the head, dyskinetic movements and generalized muscular hypotonus with spared antigravity movements but no head control and the absence of muscle tendon reflexes. Cardiac investigations were normal. EEG was abnormal with decreased background activity of the left hemisphere. Cerebrospinal fluid analysis showed increased values for Tau and neurofilament light protein. Treatment with calcium, vitamin D, coenzyme Q10, thiamine, aspartic acid, carnitine and dichloroacetate had no apparent effect on the clinical condition which continued to worsen with deteriorating liver function and increasing lactic acidosis. The serum levels of alanine transaminase increased to 62.3 U/L (ref.v. < 47.9), aspartate transaminase to 142.5 U/L (ref.v. < 53.9) and international normalized ratio to 1.4 (ref.v.<1.2). The B-lactate level increased to a maximum of 14.6 mmol/L, while pH decreased to 6.93 and base excess to – 24.9. The boy died from multi-organ failure at two months of age.

2.2. Biochemical, morphological and mtDNA studies in muscle

A muscle biopsy from the vastus lateralis of the quadriceps muscle was performed at age 2 weeks. Isolation of mitochondria, oximetric measurements on fresh mitochondria, spectrophotometric enzyme analyses, as well as muscle biopsy for ultrastructural and enzyme histochemical analyses were performed essentially as previously described [11]. Immunohistochemistry was performed with monoclonal antibodies to complex IV subunit 1 (MTCO1; Abcam; 1:4000) and a mitochondrial marker (VDAC1; Abcam; 1:2000). Long-range PCR was used to detect possible mtDNA deletions essentially as previously described [12]. To quantify mtDNA levels, a TaqMan probe-based quantitative real-time PCR was performed, as previously described [13]. The ages of the controls (1–10) at the time of biopsy were the following: 1- 1 year; 2- 1 year; 3- 10 months; 4- 5 days; 5- 2 months; 6- 2.5 months; 7- 2 months; 8- 2.5 months; 9- 3 months; 10- 14 days.

2.3. Whole-exome sequencing with data analysis and expression analysis on POLG cDNA from skeletal muscle

Whole-exome sequencing target enrichment was performed on genomic DNA extracted from skeletal muscle using the Sure SelectXT Human All Exon Kit version 6 (Agilent Technologies), and sequenced with 60 × coverage on the HiSeq4000 platform (Illumina). The 150-bp paired-end reads were aligned to the reference genome (hg19) using the CLC Biomedical Genomics workbench (Qiagen). Data were analyzed using Ingenuity Variant Analysis (IVA) (www.ingenuity.com/products/variant-analysis). We searched for candidate genes potentially associated with mitochondrial disease and included all 1158 genes listed in MitoCarta2.0 [14], and the entire mtDNA. Further filtering was done for high quality variants classified as deleterious (missense, nonsense, indel and splice-site variants +/- 10 bp around exon boundaries) and rare (<0.5% minor allele frequency in the ExAC Browser, gnomAD or 1000 Genomes). Variants of interest were further evaluated using prediction tools: PhyloP, SIFT, PolyPhen-2, and MutationTaster. Sanger sequencing was used for confirmation and segregation analysis in the parents. For equivalent quantitation of the identified POLG mutations we analyzed RNA extracted from skeletal muscle specimen by PCR and Sanger sequencing. RNA was extracted according to the manufacturer's protocol (Qiagen) and reverse-transcribed into cDNA with the QuantiTect reverse transcription kit (Qiagen). PCR reactions were carried out at 25, 27 and 29 cycles respectively for all three variants and the PCR products were sequenced using standard techniques (PCR conditions and primers are available upon request). The Sanger sequencing traces were used to estimate the mutation

load using the peak height for the mutated sequence compared to wild type allele.

2.4. Expression and purification of recombinant human proteins

Mutagenesis of POLγA was performed using the QuikChange Lightning site-directed mutagenesis kit (Agilent Technologies), and confirmed by sequencing (Eurofins MWG Operon). Recombination was performed as described in the BacPAK manual (Clontech). All versions of POLγA and all other proteins were expressed and purified as described previously [15,16].

2.5. Thermofluor stability assay

Sypro Orange (Invitrogen; $\lambda_{ex} = 490$ nm, $\lambda_{em} = 570$ nm) was used to monitor the temperature-induced unfolding of wild-type and mutant POLγA. Reactions were set up in 96-well PCR plates with POLγA (1.6 μM) and 5 × dye in assay buffer (25 mM Tris–HCl pH 8.7, 0.5 M NaCl, 0.5 mM EDTA and 10% (w/v) glycerol). Differential scanning fluorimetry was performed in a C1000 Thermal Cycler using the CFX96 real-time software (BioRad). Scans were recorded using the HEX emission filter (560–580 nm) between 4 and 95 °C in 0.5 °C increments with a 5 s equilibration time. The melting temperature (T_m) was determined from the first derivative of a plot of fluorescence intensity versus temperature [17]. Standard errors were calculated from three independent measurements.

2.6. Electrophoretic mobility shift assay (EMSA)

DNA binding affinity, $K_{d,}$ of POLγ to a 5′ ^{32}P-labelled primer-template was assayed using EMSA as previously described [18].

2.7. Coupled 3′−5′ exonuclease/polymerase assays

DNA polymerization and 3′−5′ exonuclease activities were analyzed on a 5′ ^{32}P-labelled 21-nt oligonucleotide (5′-CGG TCG AGT CTA GAG CC-3′) annealed to a 36-nt oligonucleotide (5′- TTT TAT CCG GGC TCC TCT AGA CTC GAC CG-3′). Ten μl reactions contained 10 fmol DNA template, 25 mM Tris–HCl pH 7.8, 10% glycerol, 1 mM DTT, 10 mM $MgCl_2$, 0.1 mg/ml BSA, 150 fmol wild-type or mutant POLγA, 300 fmol dimeric POLγB and the indicated concentrations of dNTPs. Reactions were incubated at 37 °C for 15 min, stopped with 15 μl gel-loading buffer (98% formamide, 10 mM EDTA, 0.025% bromophenol blue and 0.025% xylene cyanol), analyzed on 15% denaturing polyacrylamide gels in 1 × TBE, and visualized by autoradiography.

2.8. DNA synthesis

The DNA synthesis assays on ssDNA template and dsDNA template were performed as described previously [16].

2.9. Informed consent

The regional ethics committee in Gothenburg approved this study and written informed consent was obtained from the parents of the patient in the study.

3. Results

3.1. Neuroimaging studies

Brain CT and MRI performed at 2 weeks of age showed calcifications in the basal ganglia and frontal white matter (Fig. 1A). MR-spectroscopy showed an increased lactate peak in the basal ganglia and centrum semiovale (Fig. 1B).

3.2. Biochemical, morphological and mtDNA studies in muscle

The boy was referred for mitochondrial investigations at two weeks of age (Table 1). Muscle biopsy showed scattered cytochrome c oxidase (COX) negative fibers with mitochondrial proliferation (Fig. 2A i, ii, iii). These fibers were generally somewhat larger than other fibers and showed deficiency of mtDNA encoded proteins such as subunit 1 (MTCO1) of complex IV (Fig. 2A iv). qPCR analysis demonstrated depletion of mtDNA in skeletal muscle tissue, with mtDNA levels of 32% compared to ten tissue- and age-matched control samples (0–1 year of age) (Fig. 2B). No mtDNA large-scale deletions or point mutations were detected (Fig. 2C).

3.3. Whole-exome sequencing with data analysis and expression analysis on POLG cDNA from skeletal muscle

Whole-exome sequencing showed that the patient was heterozygous for three missense mutations in *POLG*, c.752C>T; p.Thr251Ile, c.1760C>T; p.Pro587Leu usually found in *cis* [19], and c.3400C>T; p.His1134Tyr. The variant c.3400C>T; p.His1134tyr with a CADD score of 28.800 was not present in the gnomAD and HGMD databases. The affected amino acid is in a highly conserved position among species with a Conservation phyloP p-value of 5.53 and is predicted to be highly pathogenic both by PolyPhen-2 with a score of 1.00 and SIFT Function Prediction. The c.3400C>T originated from the father and the *cis* mutations from the mother (Fig. 2D). Furthermore, expression analysis on *POLG* cDNA from skeletal muscle specimens revealed approximately equal amounts of transcript from both alleles, excluding the possible involvement of a promoter variant in either allele (Supplementary Fig. 1).

3.4. The p.His1134Tyr mutation is structurally disruptive

To determine pathogenicity of POLγA variants we reconstituted the mutant versions *in vitro* and assessed the effects on POLγA function. A thermofluor assay on wild-type and mutant POLγA revealed that p.His1134Tyr

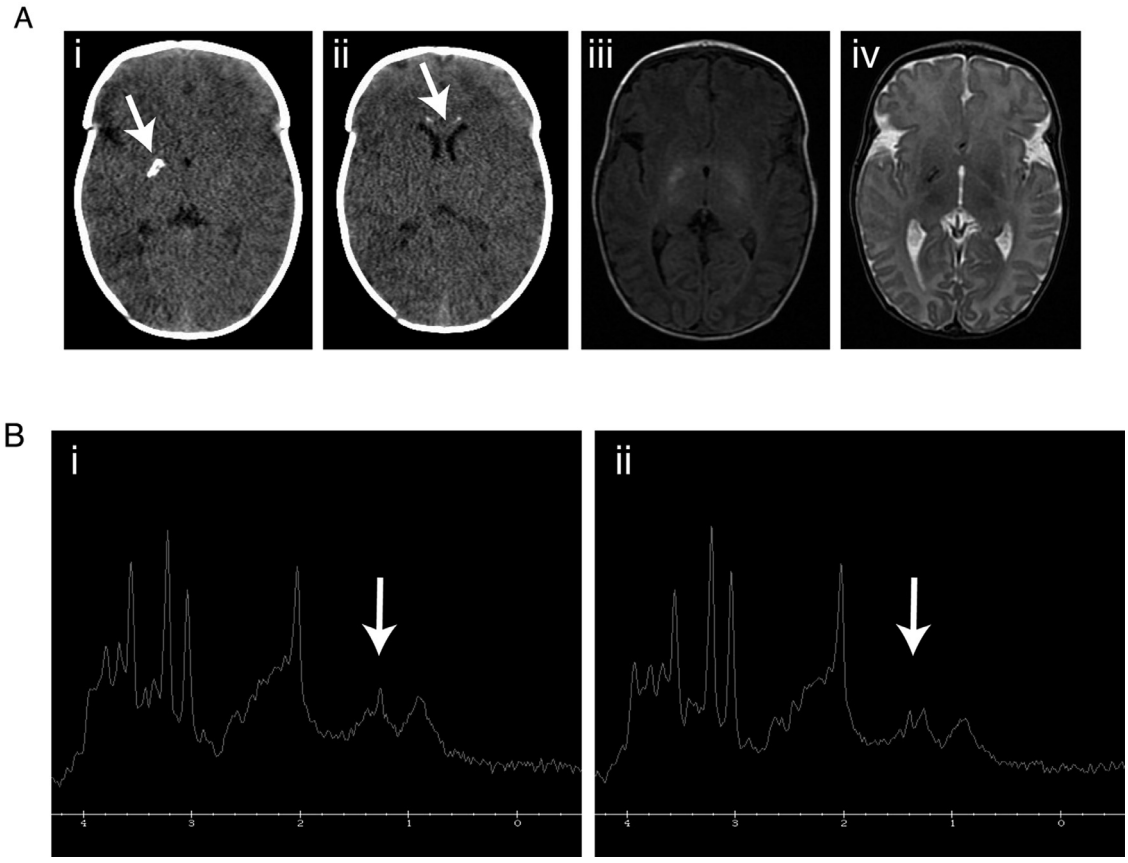

Fig. 1. **Neuroimaging at two weeks of age.** CT scan of the brain showed calcifications in globus pallidus on the right side (A-i) and medially in the frontal lobes anterior to the ventricles (A-ii). MRI of the brain with T1- and T2-weighted imaging showed corresponding signal changes but no other focal abnormalities and apparently normal myelination (A-iii and iv). MR-spectroscopy showed an increased lactate peak (arrow) in the basal ganglia and centrum semiovale (B-i and ii).

induces thermal destabilization (ΔT_m: - 2.3 °C) whereas the p.Thr251Ile/Pro587Leu double mutant shows near wild-type stability (Fig. 3A). This is in good agreement with the predicted ΔG_{unf} changes from the site directed mutator algorithm [20]. Modeling of the mutant POLγA residues (Fig. 3B) show the p.His1134Tyr mutation located within the POLγA active site where Asp890 and Glu1136 bind catalytically essential Mg^{2+}ions whilst Tyr951 and Tyr955 on the catalytic O-helix are involved in dNTP binding/recognition (Fig. 3C). A Tyr1134 residue would likely protrude into the dNTP binding pocket, causing a steric clash with the incoming dNTP and displacement of the bound Mg^{2+} ions (Fig. 3C). The Pro587 interacts closely with the POLγB accessory subunit- with a Leu587 residue causing a steric clash with the subunit- whilst the p.Thr251Ile mutation may result in the loss of two stabilizing H-bonds with Leu247 and Glu248 (Fig. 3D, E) that may cause a local structure change.

3.5. p.His1134Tyr cannot support effective DNA synthesis

To analyze the enzymatic properties of the POLγ mutants we tested their ability to bind a primed DNA template using EMSA. Both mutants bound DNA with the same affinity as wild type (Fig. 4A). Next, we conducted a coupled polymerase/exonuclease assay using the short template and different dNTP levels (Fig. 4B). The exonuclease activity of both mutants was similar to wild type (no dNTPs present, Fig. 4B, Supplementary Fig. 2A). However, p.His1134Tyr polymerization was reduced compared to p.Thr251Ile/Pro587Leu and wild type, particularly at low dNTP concentrations (Fig. 4B, lanes 7–10). On long ssDNA templates, p.His1134Tyr showed difficulty polymerizing even at high dNTP levels, whereas p.Thr251Ile/Pro587Leu behaved as wild type at all concentrations (Supplementary Fig. 2B and Fig. 4C).

To study polymerase activity within the context of the core mitochondrial replisome (POLγ, TWINKLE and, mtSSB), we performed a rolling circle assay using a double-stranded circular DNA template with a pre-formed replication fork (Fig. 5A). We used very high dNTP levels (100 μM) since p.His1134Tyr requires higher dNTP concentration than normal (Fig. 4B). Similar to our previous assays, p.Thr251Ile/Pro587Leu synthesized long DNA stretches with an efficiency comparable to wild type, whereas p.His1134Tyr was inactive despite high dNTP levels (Fig. 5B).

Our finding that the p.Thr251Ile/Pro587Leu mutation did not appear to affect POLγ activity is in direct contrast to the patient's phenotype. The patient had problems in tissues

Table 1
Laboratory investigations at diagnosis.

Biochemical investigations in blood, urine and CSF upon diagnosis with abnormal values			
S-Haemoglobin (g/L)	101 (ref>135)	CSF-lactate (mmol/L)	6.2 (ref<1.8)
S-CK (IU/L)	479 (ref<170)	CSF-Pyruvate (mmol/L)	0.18
B-Lactate (mmol/L)	4.2 (ref<1.8)	CSF-Lactate/Pyruvate ratio	35
B-Pyruvate (mmol/L)	0.18	CSF-albumin (mg/L)	4670 (ref<320)
B- Lactate/Pyruvate ratio	24	CSF/P- albumin ratio	145 (ref<6,8)
P-aminoacids	glutamine +, glycine + alanine + (valin -, leucin -, isoleucine -)	CSF-Tau protein (ng/L)	1100 (ref<250)
S-total carnitine (μmol/L)	16 (ref=23–60)	CSF- NFL (ng/L)	8790 (ref<380)
S-free carnitine (μmol/L)	11 (ref=20–55)	CSF-GFAP (ng/L)	450 (ref<450)
M-carnitine (μmol/g protein)	5.8 (ref=7.4–26)	U-Lactate (mmol/mol creatinine)	1000 (ref<40)

Muscle mitochondrial investigations							
Oximetry (nmol O x min^{-1} x mg $protein^{-1}$)			Spectrophotometry (mmol x min^{-1} x mg $protein^{-1}$)				Rate constant/*k* (min^{-1} x mg $protein^{-1}$)
Pyruvate + Malate	Succinate + Rotenone	Ascorbate + TMPD	NADH ferricyanide reductase	Succinate cytochrome-C reductase	Succinate dehydrogenase DCIP	Citrate synthase	Cytochrome-*c* oxidase
(58 - 103)	(65–113)	(174–315)	(3.5 – 7.0)	(0.14 – 0.41)	(0.15–0.36)	(1.9–3.1)	(6.1–13)
42	71	179	4.1	0.22	0.19	1.6	6.9

Abbreviations: S= serum, B= Blood, P= Plasma, M= Muscle, CSF= Cerebrospinal fluid, U= Urine, NFL= Neurofilament light chain, GFAP= Glial fibrillary acidic protein, ref = Reference value, mtDNA= Mitochondrial DNA, nDNA= Nuclear DNA, TMPD= N,N,N′,N′-Tetramethyl-p-phenylenediamine. DCIP= 2,6-Dichlorophenolindophenol (Reference values are from 10 age-matched patients (0–1 years of age) without mitochondrial disease. The reference intervals are mean ± 2SD).

with non-dividing cells, where the dNTP concentration is considerably lower [21-23] than in our rolling circle assay (Fig. 5B). We therefore decided to investigate the effect of dNTP concentration in the rolling circle assay (Fig. 5C and D). Interestingly, at more physiological (1–10 μM) dNTP concentrations and on dsDNA templates, we now saw a strong reduction in DNA synthesis also with p.Thr251Ile/Pro587Leu.

3.6. p.His1134Tyr in combination with p.Thr251Ile/Pro587Leu leads to replication stalling at low dNTP levels

To mimic the DNA replication conditions within the patient cells, we mixed equimolar amounts of p.Thr251Ile/Pro587Leu and p.His1134Tyr in rolling circle assays at physiological dNTP concentrations (1 μM). We also reconstituted the parental situation where equimolar amounts of wild type and p.Thr251Ile/Pro587Leu or p.His1134Tyr were mixed. As expected, wild type supported robust levels of rolling circle replication (Fig. 5E, lanes 2–5 and Supplementary Fig. 2C). When p.His1134Tyr was added in combination with wild type, we noted a decrease in the formation of longer replication products and increased levels of a band just above 3 kb, corresponding to the size of the input template (Fig. 5E, lanes 6–9). This effect is frequently seen with POLγ variants that have problems with processive DNA synthesis. The polymerase binds to the free 3′-end and performs an idling reaction, i.e. it switches between the polymerase and exonuclease mode, leading to a gradual increase in labeling of the input template. The effect was even more pronounced when we preincubated the template with p.His1134Tyr before wild type was added (Supplementary Fig. 2C), suggesting that p.His1134Tyr can compete with wild type for binding to the 3′-end of the primer. Mixing of p.Thr251Ile/Pro587Leu with wild type had a milder effect on replisome function (Fig. 5E, lanes 10–13 and Supplementary Fig. 2C). When p.His1134Tyr and p.Thr251Ile/Pro587Leu were added together, replication was more severely disturbed (Fig. 5E, compare lanes 2–5 with 14–17 and Supplementary Fig. 2C), with lower levels of long replication products and increased labeling of the input template. The fact that the two mutations have additive, negative effects on replication correlates well with the more severe patient phenotype.

4. Discussion

In this article, we describe a novel p.His1134Tyr mutation in the *POLG* gene which in combination with the common

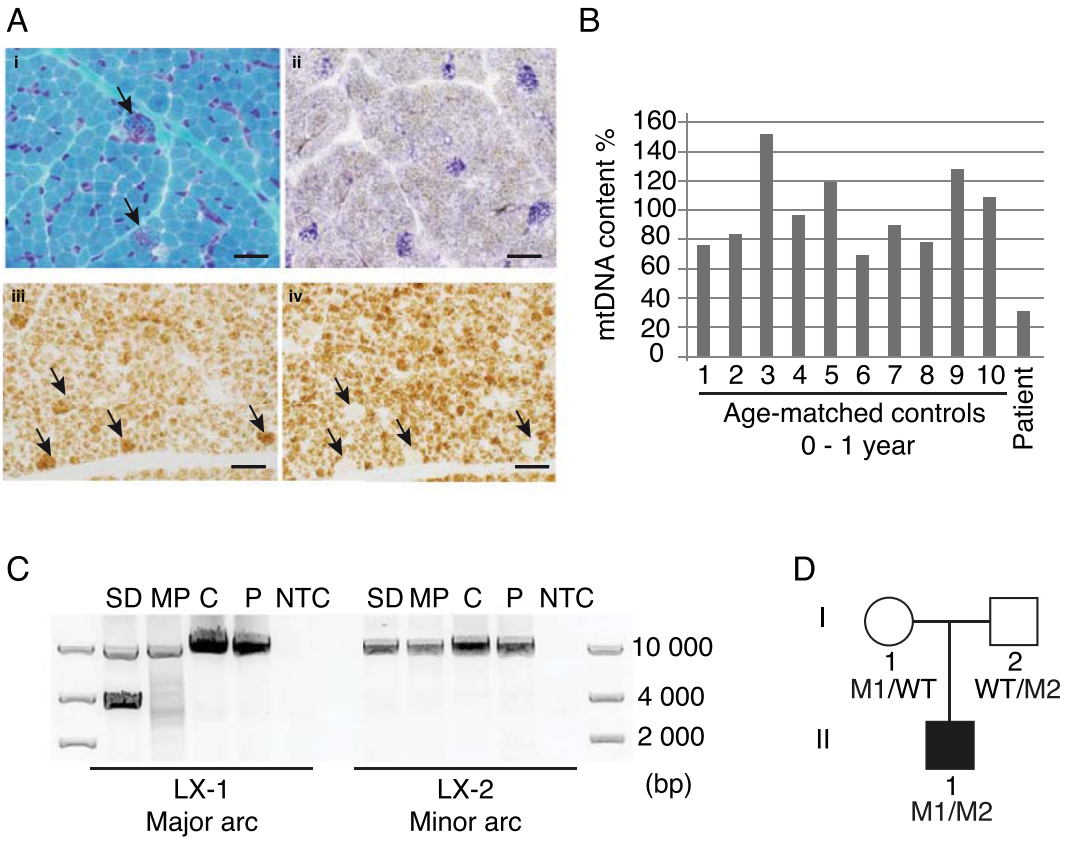

Fig. 2. **Muscle biopsy from the quadriceps muscle.** (A-i) Some large fibers show mitochondrial proliferation similar to ragged red fibers as visualized by Gomori trichrome staining (A-ii) Scattered large fibers show cytochrome c oxidase deficiency identified as blue fibers by enzyme-histochemical staining of succinate dehydrogenase and COX. (A-iii) Large fibers with mitochondrial proliferation as demonstrated with immunohistochemical staining of the mitochondrial marker VDAC1 (arrows). (A-iv) The fibers with mitochondrial proliferation in (A-iii) show immunohistochemical deficiency of mtDNA encoded complex IV, subunit 1 (MTCO1). (B) qPCR analysis showing mtDNA depletion in skeletal muscle tissue, with mtDNA levels of 32% compared to ten tissue- and age-matched control samples. (C) Long-range PCR (LX) could not detect any large-scale mtDNA deletions (SD = sample with single deletion; MP = sample with multiple deletions; C = control; P = patient; NTC = no-template control; bp = base pair). (D) Segregation analysis. M1 stands for c.752C>T; p.Thr251Ile, c.1760C>T; p.Pro587Leu and M2 is c.3400C>T; p.His1134Tyr.

p.Thr251Ile/Pro587Leu double mutant leads to a very severe and early fatal phenotype characterized by: (1) prenatal onset with intrauterine growth restriction; (2) severe muscle hypotonia and failure to thrive with lactic acidosis from birth; (3) multiorgan involvement with encephalopathy, myopathy and hepatopathy; and (4) death by two months of age. The increased cerebrospinal fluid levels of Tau and neurofilament light protein suggest ongoing neurodegeneration with cortical and white matter axonal injury [24]. Intrauterine onset has to our knowledge only been described in one previous individual with a somewhat different clinical phenotype characterized by myopathy and visceral dysmotility [10]. In Alpers syndrome, which is considered to be the most severe end of the spectrum of *POLG*-related disease, the onset is almost always after the first months of life [6,8,9, 25-27] and only rarely at birth [7].

The p.Thr251Ile/Pro587Leu double mutant is considered pathogenic and is associated with a wide range of clinical phenotypes [19]. The p.His1134Tyr mutation has not been described previously, but a compound heterozygous missense exchange of the same amino acid to arginine (p.His1134Arg) has been associated with a severe phenotype with onset at birth, early death and mtDNA depletion [25,28]. In our patient, muscle biopsy demonstrated mitochondrial myopathy with scattered COX-deficient muscle fibers and deficiency in mtDNA-encoded proteins. Dysfunction of the respiratory chain was also demonstrated in fresh, isolated muscle mitochondria. Associated with these defects we found a reduction in mtDNA copy number to 32% of age-matched controls (i.e., below the normal range), but no large-scale deletions. These results indicate that mtDNA depletion was the cause of the mitochondrial dysfunction and COX-deficient muscle fibers. There was no possibility to analyze mtDNA levels in brain or liver, but we anticipate that mtDNA depletion was also the underlying cause of disease in these organs.

The improper maintenance of mtDNA levels in the patient is in good agreement with our *in vitro* biochemical characterization of p.His1134Tyr and p.Thr251Ile/Pro587Leu POLγ. When both mutants were combined, DNA synthesis was severely affected at dNTP concentrations resembling those in non-dividing cells. The p.His1134Tyr mutant on its own showed a polymerase defect even at high

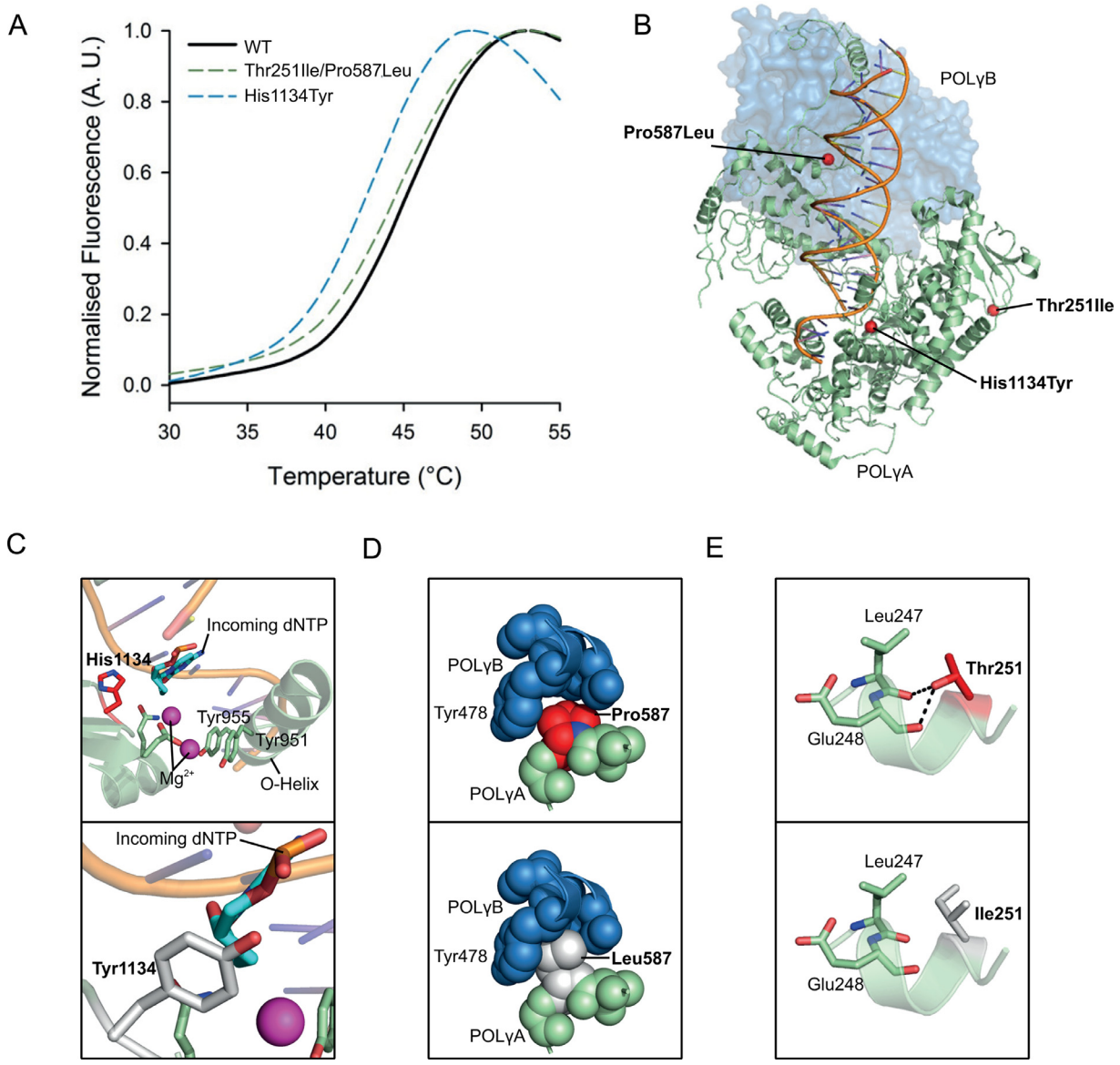

Fig. 3. **The His1134Tyr mutation is structurally disruptive.** (A) Thermofluor analysis of wild-type and mutant POLγA revealed that the p.His1134Tyr mutation induces thermal destabilization whereas p.Thr251Ile/Pro587Leu resembles the wild type. (B) The location of the Thr251Ile, Pro587Leu and His1134Tyr mutations. The Thr251Ile mutation is located in the exonuclease domain whilst the Pro587Leu mutation lies at the binding interface between POLγA and POLγB. The His1134Tyr mutation lies adjacent to the active site and in close proximity to both catalytic residues and bound DNA substrate (PDB ID: 4ZTU[30]). (C-E) The POLγ mutations were modelled on the wild type structure (PDB ID: 4ZTU[30]) using PyMol V 1.8.

dNTP concentrations. The importance of this amino acid is supported by previous work with the p.His1134Ala mutation, for which the corresponding mutation in *Drosophila melanogaster* caused developmental arrest and lethality at the larval stage [18]. His1134 is a strictly conserved amino acid located near the active site of the polymerase and contacts the template strand during replication [29,30]. A tyrosine at this position appears to protrude into the active site cavity and forms a new H-bond with Thr1071. This may limit the flexibility of the active site and impair Mg^{2+}/dNTP binding, explaining the lack of polymerase activity. The previously reported p.His1134Arg mutation also causes mtDNA depletion [25,28]. A His-to Arg-substitution will not only introduce a positive charge but also an extended side chain. Both of these properties will most likely provoke steric clashes similar to the ones seen with the change to tyrosine presented here.

The p.Thr251Ile and p.Pro587Leu mutations present *in cis* have been reported to exist in heterozygosity with a wild-type allele in ~1% of Italian controls. When present on both alleles, this mutation pair causes a relatively mild phenotype with a midlife onset [19,31,32]. In our assay conditions, p.Thr251Ile/Pro587Leu had a mild replication defect *in vitro* which is in line with phenotype in the patients. This finding contrasts with a previous report that showed that p.Thr251Ile/Pro587Leu has severely reduced

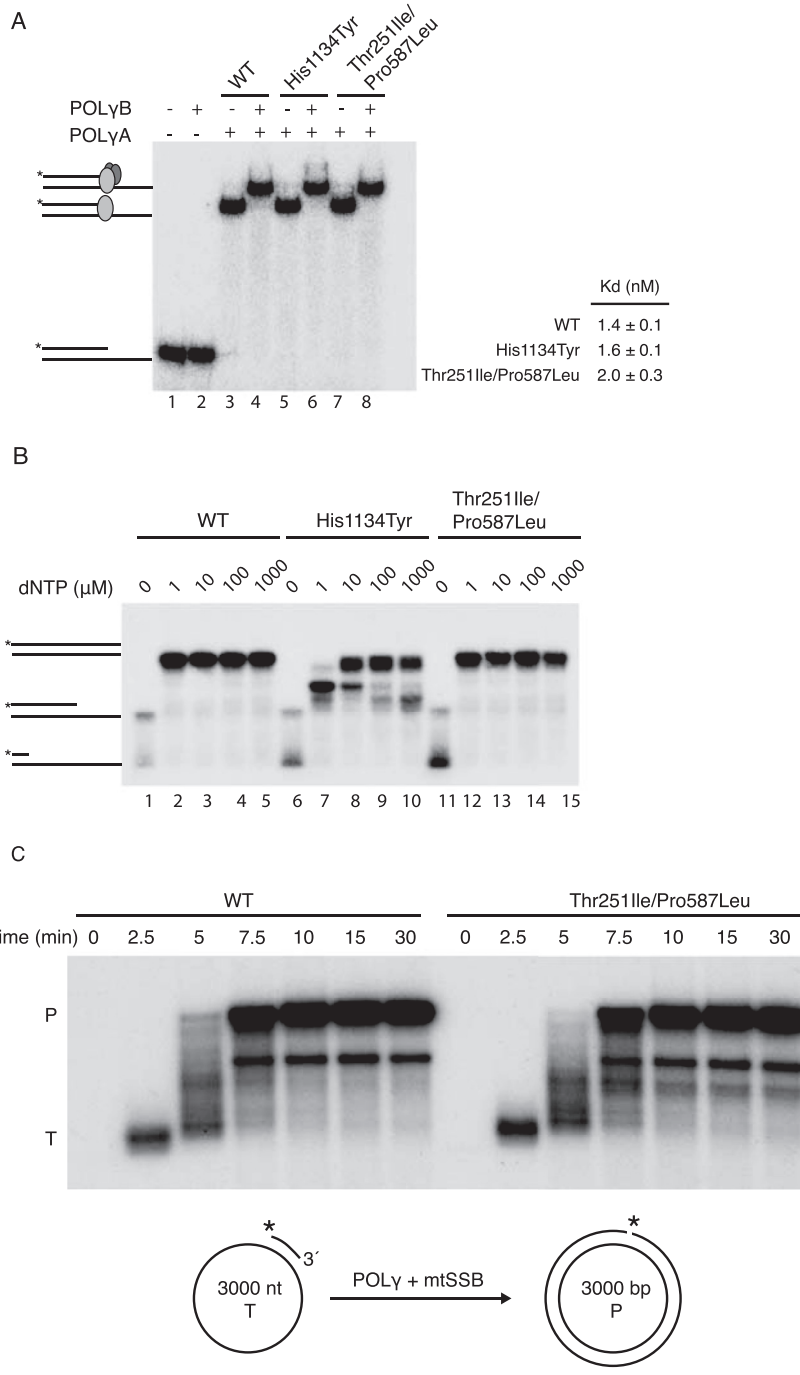

Fig. 4. **p.His1134Tyr cannot support effective DNA synthesis.** (A) The ability of wild-type and mutant POLγ to bind DNA was assayed by EMSA. The template comprised a 21-bp double-stranded region followed by a 15-nt single-stranded 3′-tail. Asterisk represents the 5′-radiolabel. The mutants bind DNA both in the absence and presence of POLγB. POLγB does not bind the template alone (lane 2). Reactions were run on a 6% native polyacrylamide gel. The K_d (DNA) values of wild type and mutant POLγ holoenzymes (POLγA/POLγB in complex) are shown to the right. Values for dissociation constants are shown as an average from at least three independent binding assays. Errors presented as s.d. (B) Coupled 3′−5′ exonuclease/polymerization assays show that the p.Thr251Ile/Pro587Leu variant has wild-type-like activity whereas p.His1134Tyr is incapable of synthesizing full-length product even at high dNTP concentrations. Reactions were run on a 15% denaturing polyacrylamide gel. The 5′-labelled template, used for both experiments, is shown alongside each gel. (C) DNA synthesis assay using a long circular ssDNA template of 3000 nt at 2.5 μM shows that the p.Thr251Ile/Pro587Leu variant has wild-type-like activity on ssDNA templates. T stands for ssDNA template and P for product.

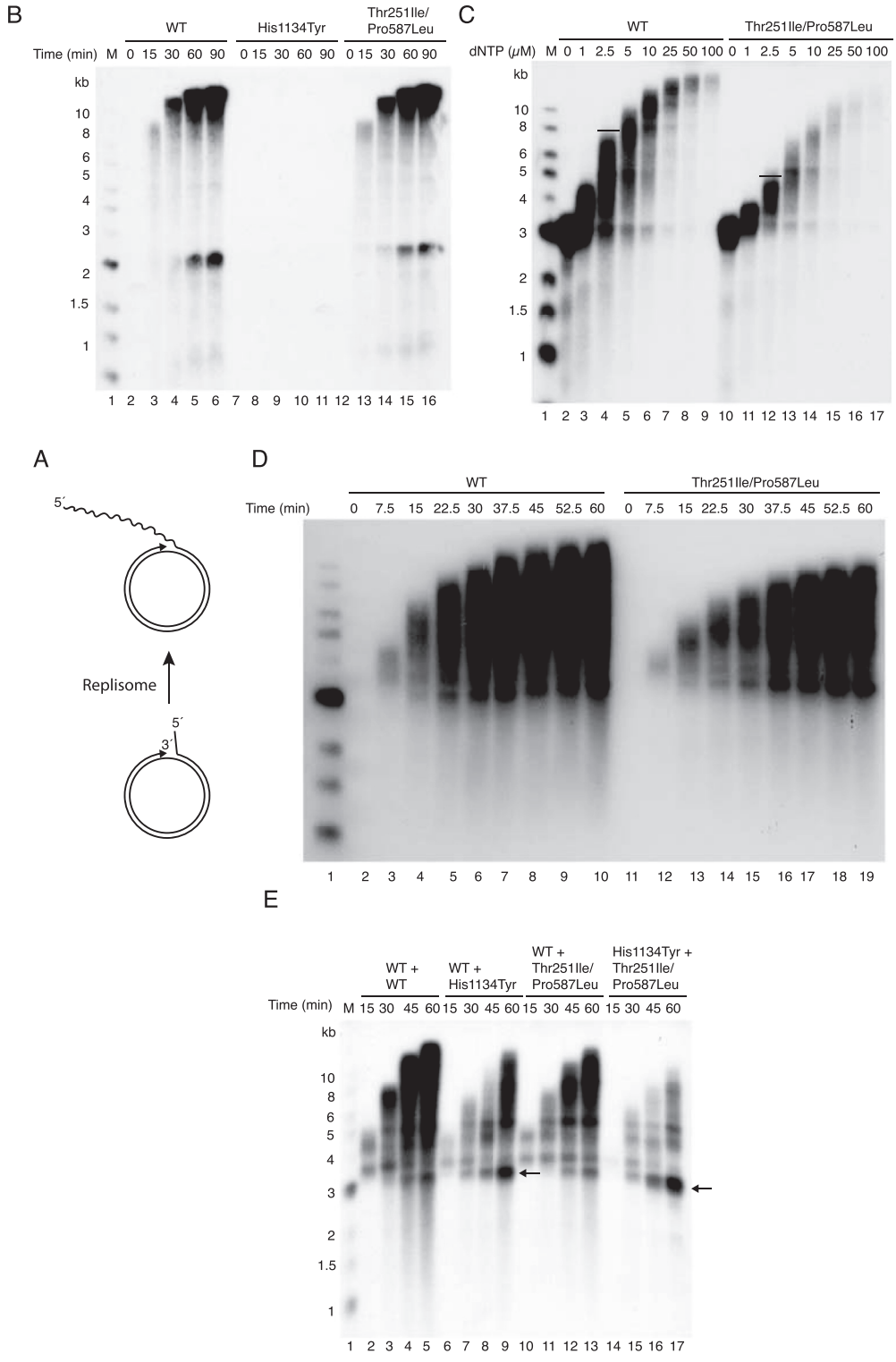

Fig. 5. **POLγ mutants affect DNA replication at low dNTP concentrations**. (A) Schematic of assay showing the rolling-circle template. (B) A rolling circle replication assay (100 μM dNTP) demonstrates that p.Thr251Ile/Pro587Leu synthesizes long DNA stretches with efficiency comparable to wild type (lanes 12–16) whereas p.His1134Tyr is catalytically inactive (lanes 7–11). (C) Interestingly, p.Thr251Ile/Pro587Leu shows a more pronounced dNTP concentration-dependent inhibition of its activity as compared to the wild type. The bars shown indicate equivalent time points for the wild type and p.Thr251Ile/Pro587Leu for comparison. Reactions run for 30 min. (D) A time-course experiment performed with 2.5 μM dNTPs reveals a distinct difference in DNA synthesis efficiency between wild type and p.Thr251Ile/Pro587Leu. (E) A mixing experiment with indicated combinations of the POLG variants at 1 μM dNTPs. At low (1 μM) dNTP levels, p.His1134Tyr displays a negative effect over both wild type and p.Thr251Ile/Pro587Leu (compare lanes 2–5 with 6–9 and lanes 10–13 with 14–17). The very strong inhibition of replication observed when mixing p.His1134Tyr and p.Thr251Ile/Pro587Leu (lanes 14–17) correlates well with the severe patient phenotype. The arrow indicates stalled replication products due to the presence of the p.His1134Tyr mutant.

catalytic activity [31]. The p.Thr251Ile/Pro587Leu mutant failed to efficiently support DNA replication on dsDNA, i.e. when the polymerase acts together with TWINKLE and the defect is more pronounced at physiological dNTP concentrations (Fig. 5C and D). Neither the Thr251Ile nor Pro587Leu mutations are close to the polymerase active site. Thr251 is located in the exonuclease domain whereas Pro587 is a conserved residue in the linker domain at the interface between POLγA and POLγB [31]. Interestingly, the molecular defects observed with p.Thr251Ile/Pro587Leu are similar to those previously described for mutations in POLγB ($Arg_{328}Lys_{329}$ and $Arg_{363}Lys_{364}Lys_{365}$), which efficiently performs DNA synthesis on ssDNA, but fails to support replisome function on a dsDNA template [1,33]. It is therefore possible that p.Thr251Ile/Pro587Leu does not affect the polymerase activity *per se*, but affects POLγ activity in the context of the replisome, potentially disturbing functional interactions with TWINKLE.

The p.His1134Tyr mutation seems to have a mild inhibitory effect also in combination with wild type. The inhibitory effect of p.His1134Tyr is likely due to its wild type-like DNA binding ability (Fig. 4A). This means that p.His1134Tyr can compete for the primer and thereby inhibit functional DNA synthesis (seen as the 3 kb stalled product in Fig. 5E and Supplementary Fig. 2C). Apparently, this defect is not sufficiently strong to generate a disease phenotype in the father.

5. Conclusion

In summary, we have identified a novel p.His1134Tyr mutation in POLγA which, in *trans* with the p.Thr251Ile/Pro587Leu double mutant, causes a distinct and severe molecular phenotype. Whereas the combination of p.Thr251Ile/Pro587Leu with other recessive POLγA mutations often causes adult-onset mitochondrial pathologies [34-36], the combination with p.His1134Tyr is associated with intrauterine onset of disease with clinical features at birth. When combined, p.His1134Tyr and p.Thr251Ile/Pro587Leu cause a very severe phenotype *in vitro*, which can be substantially improved in the presence of higher dNTP concentrations. Deoxynucleoside combination therapy has a positive effect on patients with TK2 deficiency and our data suggest that a similar therapeutic approach can be beneficial for patients with certain disease-causing POLγ variants [37].

Declaration of Competing Interest

The authors declare that they have no known competing financial interests or personal relationships that could have appeared to influence the work reported in this paper.

Acknowledgments

We are grateful to Dr. Jay P. Uhler who helped to prepare the illustrations and to coordinate the manuscript. This work was supported by the Swedish Research Council (MF and AO); Swedish Cancer Foundation (MF); European Research Council (MF); the IngaBritt and Arne Lundberg Foundation (MF); the Knut and Alice Wallenbergs Foundation (MF); AnnMari and Per Ahlqvist Foundation (ND). Västra Götalands Regionen to M.F. (ALFGBG-727491), N.D. (ALFGBG-718681) and A.O. (ALFGBG-716821).

Supplementary materials

Supplementary material associated with this article can be found, in the online version, at doi:10.1016/j.nmd.2021.01.004.

References

[1] Lee YS, Kennedy WD, Yin YW. Structural insight into processive human mitochondrial DNA synthesis and disease-related polymerase mutations. Cell 2009;139:312–24. doi:10.1016/j.cell.2009.07.050.
[2] Clayton DA. Structure and function of the mitochondrial genome. J Inherit Metab Dis 1992;15:439–47. doi:10.1007/Bf01799602.
[3] Young MJ, Copeland WC. Human mitochondrial DNA replication machinery and disease. Curr Opin Genet Dev 2016;38:52–62. doi:10.1016/j.gde.2016.03.005.
[4] Chinnery PF, Zeviani M. 155th ENMC workshop: polymerase gamma and disorders of mitochondrial DNA synthesis, 21-23 September 2007, Naarden, The Netherlands. Neuromuscul Disord 2008;18:259–67. doi:10.1016/j.nmd.2007.11.005.
[5] Falkenberg M, Larsson NG, Gustafsson CM. DNA replication and transcription in mammalian mitochondria. Annu Rev Biochem 2007;76:679–99. doi:10.1146/annurev.biochem.76.060305.152028.
[6] Ferrari G, Lamantea E, Donati A, Filosto M, Briem E, Carrara F, et al. Infantile hepatocerebral syndromes associated with mutations in the mitochondrial DNA polymerase-gammaA. Brain 2005;128:723–31. doi:10.1093/brain/awh410.
[7] Davidzon G, Mancuso M, Ferraris S, Quinzii C, Hirano M, Peters HL, et al. POLG mutations and Alpers syndrome. Ann Neurol 2005;57:921–3. doi:10.1002/ana.20498.
[8] Naviaux RK, Nguyen KV. POLG mutations associated with Alpers' syndrome and mitochondrial DNA depletion. Ann Neurol 2004;55:706–12. doi:10.1002/ana.20079.
[9] Sofou K, Moslemi AR, Kollberg G, Bjarnadottir I, Oldfors A, Nennesmo I, et al. Phenotypic and genotypic variability in Alpers syndrome. Eur J Paediatr Neurol 2012;16:379–89. doi:10.1016/j.ejpn.2011.12.006.
[10] Giordano C, Powell H, Leopizzi M, De Curtis M, Travaglini C, Sebastiani M, et al. Fatal congenital myopathy and gastrointestinal pseudo-obstruction due to POLG1 mutations. Neurology 2009;72:1103–5. doi:10.1212/01.wnl.0000345002.47396.e1.
[11] Tulinius MH, Holme E, Kristiansson B, Larsson NG, Oldfors A. Mitochondrial encephalomyopathies in childhood. I. Biochemical and morphologic investigations [see comments]. J Pediatr 1991;119:242–50. doi:10.1016/s0022-3476(05)80734-6.
[12] Moslemi AR, Melberg A, Holme E, Oldfors A. Autosomal dominant progressive external ophthalmoplegia: distribution of multiple mitochondrial DNA deletions. Neurology 1999;53:79–84. doi:10.1212/Wnl.53.1.79.
[13] Roos S, Macao B, Fuste JM, Lindberg C, Jemt E, Holme E, et al. Subnormal levels of POLgammaA cause inefficient initiation of light-strand DNA synthesis and lead to mitochondrial DNA deletions and progressive external ophthalmoplegia [corrected]. Hum Mol Genet 2013;22:2411–22. doi:10.1093/hmg/ddt094.
[14] Calvo SE, Clauser KR, Mootha VK. MitoCarta2.0: an updated inventory of mammalian mitochondrial proteins. Nucl Acids Res 2016;44:D1251–7. doi:10.1093/nar/gkv1003.

[15] Korhonen JA, Pham XH, Pellegrini M, Falkenberg M. Reconstitution of a minimal mtDNA replisome in vitro. EMBO J 2004;23:2423–9. doi:10.1038/sj.emboj.7600257.
[16] Hedberg-Oldfors C, Macao B, Basu S, Lindberg C, Peter B, Erdinc D, et al. Deep sequencing of mitochondrial DNA and characterization of a novel POLG mutation in a patient with arPEO. Neurol Genet 2020;6:e391. doi:10.1212/nxg.0000000000000391.
[17] Matulis D, Kranz JK, Salemme FR, Todd MJ. Thermodynamic stability of carbonic anhydrase: measurements of binding affinity and stoichiometry using ThermoFluor. Biochemistry 2005;44:5258–66. doi:10.1021/bi048135v.
[18] Bratic A, Kauppila TE, Macao B, Gronke S, Siibak T, Stewart JB, et al. Complementation between polymerase- and exonuclease-deficient mitochondrial DNA polymerase mutants in genomically engineered flies. Nat Commun 2015;6:8808. doi:10.1038/ncomms9808.
[19] Scuderi C, Borgione E, Castello F, Lo Giudice M, Santa Paola S, Giambirtone M, et al. The in cis T251I and P587L POLG1 base changes: description of a new family and literature review. Neuromuscul Disord 2015;25:333–9. doi:10.1016/j.nmd.2015.01.004.
[20] Topham CM, Srinivasan N, Blundell TL. Prediction of the stability of protein mutants based on structural environment-dependent amino acid substitution and propensity tables. Protein Eng 1997;10:7–21. doi:10.1093/protein/10.1.7.
[21] Ferraro P, Nicolosi L, Bernardi P, Reichard P, Bianchi V. Mitochondrial deoxynucleotide pool sizes in mouse liver and evidence for a transport mechanism for thymidine monophosphate. Proc Natl Acad Sci USA 2006;103:18586–91. doi:10.1073/pnas.0609020103.
[22] Kong ZQ, Jia SD, Chabes AL, Appelblad P, Lundmark R, Moritz T, et al. Simultaneous determination of ribonucleoside and deoxyribonucleoside triphosphates in biological samples by hydrophilic interaction liquid chromatography coupled with tandem mass spectrometry. Nucl Acids Res 2018;46:e66. doi:10.1093/nar/gky203.
[23] Wheeler LJ, Mathews CK. Nucleoside triphosphate pool asymmetry in mammalian mitochondria. J Biol Chem 2011;286:16992–6. doi:10.1074/jbc.M111.236968.
[24] Shahim P, Mansson JE, Darin N, Zetterberg H, Mattsson N. Cerebrospinal fluid biomarkers in neurological diseases in children. Eur J Paediatr Neurol 2013;17:7–13. doi:10.1016/j.ejpn.2012.09.005.
[25] Hikmat O, Tzoulis C, Chong WK, Chentouf L, Klingenberg C, Fratter C, et al. The clinical spectrum and natural history of early-onset diseases due to DNA polymerase gamma mutations. Genet Med 2017;19:1217–25. doi:10.1038/gim.2017.35.
[26] Horvath R, Hudson G, Ferrari G, Futterer N, Ahola S, Lamantea E, et al. Phenotypic spectrum associated with mutations of the mitochondrial polymerase gamma gene. Brain 2006;129:1674–84. doi:10.1093/brain/awl088.
[27] Isohanni P, Hakonen AH, Euro L, Paetau I, Linnankivi T, Liukkonen E, et al. POLG1 manifestations in childhood. Neurology 2011;76:811–15. doi:10.1212/WNL.0b013e31820e7b25.
[28] Taanman JW, Rahman S, Pagnamenta AT, Morris AA, Bitner-Glindzicz M, Wolf NI, et al. Analysis of mutant DNA polymerase gamma in patients with mitochondrial DNA depletion. Hum Mutat 2009;30:248–54. doi:10.1002/humu.20852.
[29] Farnum GA, Nurminen A, Kaguni LS. Mapping 136 pathogenic mutations into functional modules in human DNA polymerase gamma establishes predictive genotype-phenotype correlations for the complete spectrum of POLG syndromes. Biochim Biophys Acta 2014;1837:1113–21. doi:10.1016/j.bbabio.2014.01.021.
[30] Szymanski MR, Kuznetsov VB, Shumate C, Meng Q, Lee YS, Patel G, et al. Structural basis for processivity and antiviral drug toxicity in human mitochondrial DNA replicase. EMBO J 2015;34:1959–70. doi:10.15252/embj.201591520.
[31] DeBalsi KL, Longley MJ, Hoff KE, Copeland WC. Synergistic effects of the in cis T251I and P587L mitochondrial dna polymerase gamma disease mutations. J Biol Chem 2017;292:4198–209. doi:10.1074/jbc.M116.773341.
[32] Tang S, Wang J, Lee NC, Milone M, Halberg MC, Schmitt ES, et al. Mitochondrial DNA polymerase gamma mutations: an ever expanding molecular and clinical spectrum. J Med Genet 2011;48:669–81. doi:10.1136/jmedgenet-2011-100222.
[33] Farge G, Pham XH, Holmlund T, Khorostov I, Falkenberg M. The accessory subunit B of DNA polymerase gamma is required for mitochondrial replisome function. Nucl Acids Res 2007;35:902–11. doi:10.1093/nar/gkl1116.
[34] Kollberg G, Jansson M, Perez-Bercoff A, Melberg A, Lindberg C, Holme E, et al. Low frequency of mtDNA point mutations in patients with PEO associated with POLG1 mutations. Eur J Hum Genet 2005;13:463–9. doi:10.1038/sj.ejhg.5201341.
[35] Weiss MD, Saneto RP. Sensory ataxic neuropathy with dysarthria and ophthalmoparesis (SANDO) in late life due to compound heterozygous POLG mutations. Muscle Nerve 2010;41:882–5. doi:10.1002/mus.21636.
[36] Lovan A, Ihtsham ul H, Balakrishnan N. Diagnostic challenges in movement disorders: sensory Ataxia Neuropathy Dysarthria and Ophthalmoplegia (SANDO) syndrome. BMJ Case Rep 2013;2013. doi:10.1136/bcr-2013-010343.
[37] Lopez-Gomez C, Levy RJ, Sanchez-Quintero MJ, Juanola-Falgarona M, Barca E, Garcia-Diaz B, et al. Deoxycytidine and deoxythymidine treatment for thymidine kinase 2 deficiency. Ann Neurol 2017;81:641–52. doi:10.1002/ana.24922.